Am J Physiol Renal Physiol 282: F877–F885, 2002;
10.1152/ajprenal.00171.2001.

Confocal imaging of organic anion transport in intact rat choroid plexus

CHRISTOPHER M. BREEN,[1] DESTINY B. SYKES,[1] GERT FRICKER,[2] AND DAVID S. MILLER[1]
[1]*Laboratory of Pharmacology and Chemistry, National Institute of Environmental Health Sciences, National Institutes of Health, Research Triangle Park, North Carolina 27709; and* [2]*Institut fur Pharmazeutische Technologie und Biopharmazie, INF 366, D-69120 Heidelberg, Germany*

Received 30 May 2001; accepted in final form 20 November 2001

Breen, Christopher M., Destiny B. Sykes, Gert Fricker, and David S. Miller. Confocal imaging of organic anion transport in intact rat choroid plexus. *Am J Physiol Renal Physiol* 282: F877–F885, 2002; 10.1152/ajprenal.00171.2001.—We used confocal microscopy and quantitative image analysis to follow the movement of the fluorescent organic anion fluorescein (FL) from bath to cell and cell to blood vessel in intact rat lateral choroid plexus. FL accumulation in epithelial cells and underlying vessels was rapid, concentrative, and reduced by other organic anions. At steady state, cell fluorescence exceeded bath fluorescence by a factor of 3–5, and vessel fluorescence exceeded cell fluorescence by a factor of ~2. In cells, FL distributed between diffuse and punctate compartments. Cell and vessel accumulation of FL decreased when metabolism was inhibited by KCN, when bath Na^+ was reduced from 130 to 26 mM, and when the Na^+ gradient was collapsed with ouabain. Cell and vessel accumulation increased by >50% when 1–10 μM glutarate was added to the bath. Finally, transport of FL and carboxyfluorescein (generated intracellularly from carboxyfluorescein diacetate) from cell to blood vessel was greatly diminished when medium K^+ concentration ($[K^+]$) was increased 10-fold. These results *1*) validate a new approach to the study of choroid plexus function, and *2*) indicate a two-step mechanism for transepithelial organic anion transport: indirect coupling of uptake to Na^+ at the apical membrane and electrical potential-driven efflux at the basolateral membrane.

transepithelial transport; potential-driven efflux; blood-brain barrier; 2,4-dichlorophenoxyacetic acid; fluorescein

THE CHOROID PLEXUS together with brain capillaries constitutes the blood-brain barrier, which regulates the fluid environment of the central nervous system (CNS) and protects the tissue from potentially toxic chemicals. In many respects, the choroid plexus functions as the "kidney of the brain," producing cerebrospinal fluid (CSF), absorbing nutrients from the blood, and removing xenobiotics, xenobiotic metabolites, and waste products of metabolism from the CNS for subsequent excretion in bile and urine. Like the renal proximal tubule and the liver, the choroid plexus possesses one or more potent excretory transport systems for organic anions. A number of small organic anions are substrates for transport; these include neurotransmitter metabolites [5-hydroxyindoleacetic acid (4, 26)], drugs such as penicillin (22, 23), and environmental pollutants including 2,4-dichlorophenoxyacetic acid (2,4-D; Ref. 18). Recent experiments with isolated apical membrane vesicles from choroid plexus and with choroid plexus slices show that 2,4-D uptake at the apical membrane is driven by indirect coupling to Na^+ through organic anion dicarboxylate exchange and Na^+-dicarboxylate cotransport (20). However, nothing is known about how organic anions are distributed within the tissue and what processes drive the exit step at the basolateral membrane.

Small size, inaccessible location, and morphological complexity limit our ability to characterize and study the mechanisms responsible for transport in intact mammalian choroid plexus. Twenty-five years ago, Bresler and colleagues (1) used fluorescence microscopy to demonstrate that the small fluorescent organic anion fluorescein (FL) accumulated within choroid plexus tissue. More recently, confocal microscopy and quantitative image analysis have been used to define mechanisms of organic anion transport in renal proximal tubule (10, 12). In the present study, we employed these techniques to examine the mechanisms responsible for transepithelial transport of FL in intact rat choroid plexus. Our images show that a two-step mechanism drives transepithelial organic anion transport. One step is Na^+-dependent uptake at the apical (CNS side) plasma membrane. The second step is electrical potential difference (PD)-driven efflux from the cells at the basolateral membrane. These are the first experiments to demonstrate uphill transepithelial organic anion transport in choroid plexus in vitro and the first to shed light on events at the basolateral membrane.

MATERIALS AND METHODS

Chemicals. FL and carboxyfluorescein diacetate (CFDA) were obtained from Molecular Probes. [^{3}H]2,4-D was obtained from American Radiolabeled Chemicals. All other chemicals were of reagent grade or better and were obtained from commercial suppliers.

Address for reprint requests and other correspondence: D. S. Miller, LPC, NIH/NIEHS, P.O. Box 12233, Research Triangle Park, NC 27709 (E-mail: miller@niehs.nih.gov).

The costs of publication of this article were defrayed in part by the payment of page charges. The article must therefore be hereby marked "*advertisement*" in accordance with 18 U.S.C. Section 1734 solely to indicate this fact.

Animals. Adult male Sprague-Dawley rats (body wt 250–400 g) were obtained from Taconic Farms and were euthanized with CO_2. The top of the cranium was removed and the lateral choroid plexus was isolated using a Dumont no. 5 forceps inserted into each hemisphere. Tissue was immediately transferred to ice-cold artificial cerebrospinal fluid (aCSF) that contained (in mM) 103 NaCl, 4.7 KCl, 2.5 $CaCl_2$, 1.2 KH_2PO_4, 1.2 $MgSO_4$, 25 $NaHCO_3$, 10 glucose, and 1 sodium pyruvate at pH 7.4 and was previously gassed with 95% O_2-5% CO_2.

Confocal imaging. For imaging experiments, each plexus was divided into two pieces and each piece was transferred to a covered Teflon incubation chamber that contained 1.0 ml of pregassed aCSF with 0.5–1 μM FL and added effectors. The chamber floor was a 4 × 4-cm glass coverslip to which the tissue adhered lightly and through which it could be viewed by means of an inverted microscope. Fluorescent compounds and inhibitors were added to the incubation medium as stock solutions in aCSF or DMSO. Preliminary experiments showed that the final concentrations of DMSO used (≤0.5%) had no significant effects on the uptake and distribution of FL or the uptake of 2,4-D. All transport experiments were conducted at room temperature (18–20°C) and all chambers with tissue were maintained in Ziploc plastic bags containing 95% O_2-5% CO_2 under slight positive pressure until being removed for confocal imaging.

To acquire images, the chamber containing the tissue was mounted on the stage of a Zeiss inverted confocal laser-scanning microscope (model 510 or 410) and viewed through a ×40 water-immersion objective (numeric aperture = 1.2). A 488-nm laser line (Ar-ion laser), a 505-nm dichroic filter, and a 510-nm long-pass emission filter were used. Low laser intensity was used to avoid photobleaching. With the photomultiplier gain set to yield an average cellular fluorescence intensity of 50–100 U (full scale = 255 U), tissue autofluorescence was undetectable. Tissue was viewed under reduced transmitted-light illumination. An area including undamaged epithelium and the underlying blood vessel was selected, and a confocal fluorescence image (512 × 512 × 8 bits) was acquired and saved to disk. Fluorescence intensities were measured from stored images using Zeiss Image Analyzer software, National Institutes of Health Image 1.61, or Scion Image software as described previously (12). From each piece of tissue under investigation, 5–10 areas of epithelium and adjacent vasculature were selected for measurement. The background fluorescence intensity was subtracted, and the average pixel intensity for each area was calculated. Although some preparation-to-preparation variation in transport ability was noted, most of the differences in fluorescence intensities for control tissue reflect changes in photomultiplier gain settings. Data shown are results of single experiments that are representative of two to four experiments.

Initial experiments showed that at the photomultiplier gain settings used, measured fluorescence intensity was a linear function of FL concentration (up to 20 μM). However, because there are uncertainties in relating cellular fluorescence to the actual concentration of an accumulated compound in cells and tissues with complex geometry, data are reported here as average measured pixel intensity rather than estimated dye concentration.

Tracer uptake. For radiolabel-uptake experiments, whole plexuses were removed to aCSF maintained at 37°C and gassed with 95% O_2-5% CO_2. Plexuses were then transferred to aCSF containing 10 μM [^{3}H]2,4-D and added effectors. After 5 min, the tissue was removed, rinsed, blotted, weighed, and counted. Tissue uptake was calculated as the tissue-to-medium ratio [disintegrations/min (dpm)/mg of tissue divided by dpm/μl of medium].

Statistics. Data are presented as means ± SE. Means were compared using Student's *t*-test or one-way ANOVA followed by Dunnett's post-test using Prism software. Values were deemed to be significantly different when $P < 0.05$.

RESULTS

Figure 1 shows transmitted light and confocal micrographs of choroid plexus tissue after 30 min of incubation in aCSF containing 1 μM FL. In the transmitted-light image, the apical brush-border membrane appears as a refractile element between cells and medium (Fig. 1*A*). The epithelial cells contain a large central nucleus and smaller organelles. Beneath the epithelium is an interstitial space, a perivascular space, and a blood vessel containing red cells. Unlike most other capillaries in the brain, those in choroid plexus are fenestrated and thus the endothelium should be no barrier to exchange of solutes between the vasculature and the interstitial/perivascular spaces.

The confocal slice shows that FL accumulated in both the epithelial cells and the interstitial/perivascular/vascular spaces (Fig. 1*B*). Fluorescence intensity in the cells is clearly greater than in the medium, and fluorescence intensity in the perivascular and vascular spaces is greater than in the cells, which indicates a two-step mechanism of transepithelial transport. Within the cells, fluorescence is distributed in both diffuse and punctate compartments (Fig. 1, *B* and *C*), which suggests sequestration within vesicular structures as seen previously for organic cations in choroid plexus (16) and for organic anions in renal proximal tubule (14, 15). Nuclear fluorescence appears to be lower than diffuse cytoplasmic fluorescence (Fig. 1*C*). Because the nucleus contains no vesicular organelles and because the nuclear envelope should be no barrier to diffusion of a small molecule such as FL, nuclear levels may be an indicator of fluorescence intensity in organelle-free cytoplasm.

Within the blood vessels, red cells can be seen as areas of very low fluorescence, thereby indicating exclusion of FL from these cells or quenching of fluorescence by hemoglobin (Fig. 1*B*). Despite the low fluorescence within red cells, spaces between and around these cells are highly fluorescent, i.e., roughly equivalent to the perivascular space. Figure 2 shows a single slice from a stack of confocal images (*z*-series) as well as *z*-sections cut at right angles through the stack. The *z*-sections show that high levels of fluorescence extend from the base of the epithelial cells up toward the tight junctions at the apex of the lateral intercellular spaces. This high level of fluorescence often fills a continuous space extending from the interstitial space below the tight junctions to the interior of the blood vessels. A sense of the three-dimensional relationships among tissue elements can be obtained by viewing the stereo images in Fig. 3.

Figure 4 shows the time course of FL accumulation in choroid plexus epithelial cells and vascular spaces. For comparison, medium fluorescence in this experiment was 25 U. Both cellular and vascular fluorescence

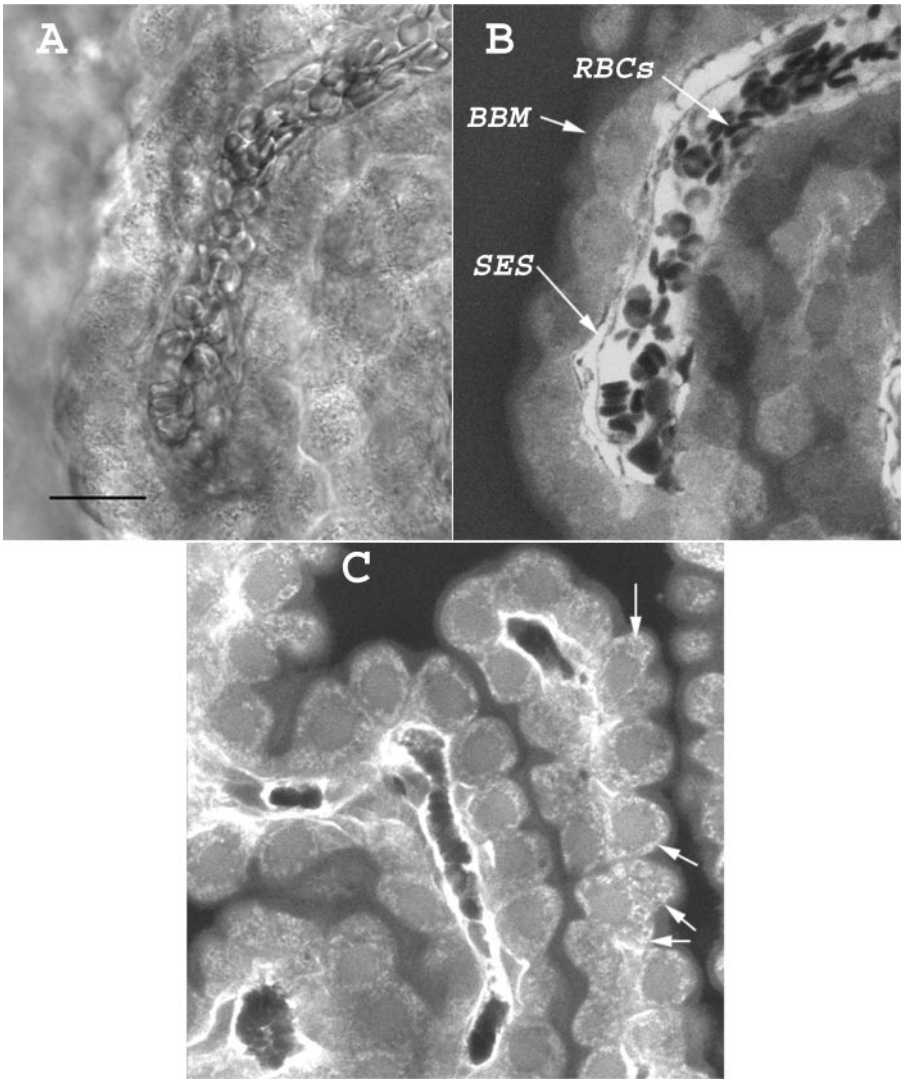

Fig. 1. Transmitted light (*A*) and confocal (*B*, *C*) images of rat choroid plexus after 30-min incubation in medium with 1 μM fluorescein (FL). Confocal slices were acquired at different gain settings: in *B*, gain was adjusted to give an image in which vascular fluorescence intensity averaged 150–200 U. This is a control image similar to those used for quantitation of fluorescence. Gain in *C* was raised to emphasize the nonuniform distribution of fluorescence within epithelial cells as well as the intense fluorescence within the perivascular and vascular spaces. Black scale bar (*A*), 20 μm. RBCs, red cells in a blood vessel; BBM, brush border (apical) membrane; SES, subepithelial space. Arrows (*C*) indicate regions of punctate fluorescence.

increased rapidly over the first 20 min and reached steady-state values within 30 min. Initially, cellular fluorescence exceeded vascular fluorescence, but at steady state, vascular fluorescence > cellular fluorescence > medium fluorescence (Fig. 4). Other experiments (not shown) indicated that tissue levels of fluorescence did not decline over incubation periods of 1–2 h.

Experiments in which steady-state levels of fluorescence were measured indicate that FL transport was metabolism dependent and specific. Inhibiting metabolism with KCN reduced cellular and vascular fluorescence by 75% (Fig. 5). Addition of the organic anions probenecid (10 μM) or 2,4-D (25 μM) to the medium also substantially reduced cellular and vascular fluorescence. p-Aminohippurate (PAH) at 100 μM was much less effective in that it only reduced cellular accumulation of FL by ~30% and did not significantly affect vessel fluorescence. PAH appears to be a poor inhibitor of organic anion transport in choroid plexus (20), and it is possible that in these experiments PAH did not attain a high enough concentration within choroid plexus cells to affect the exit step of FL transport. Leukotriene C_4 (LTC_4) was without effect (Fig. 5).

Previous studies using isolated apical membrane vesicles from choroid plexus and choroid plexus slices have shown that transport of the anionic herbicide 2,4-D across the apical membrane is indirectly coupled to the Na^+ gradient (20). Energetic coupling was through Na^+-dicarboxylate cotransport and 2,4-D/dicarboxylate exchange. Thus transport in intact tissue could be inhibited by treatments that reduced the Na^+ gradient (Na^+ depletion and ouabain) and stimulated by treatments that increased the dicarboxylate gradient [incubation with glutarate, a nonmetabolizable analog of α-ketoglutarate, which rapidly accumulates intracellularly (20)]. Figure 6 shows that replacing one-half of the NaCl in aCSF did not affect FL transport but that replacing all of the NaCl (Na^+ concentration of 25 mM due to $NaHCO_3$) significantly reduced cellular and luminal fluorescence. Ouabain, an inhibitor of Na,K-ATPase, also significantly reduced cellular and vascular fluorescence (Fig. 6). With 5 mM ouabain, cellular fluorescence decreased by 60% and vascular

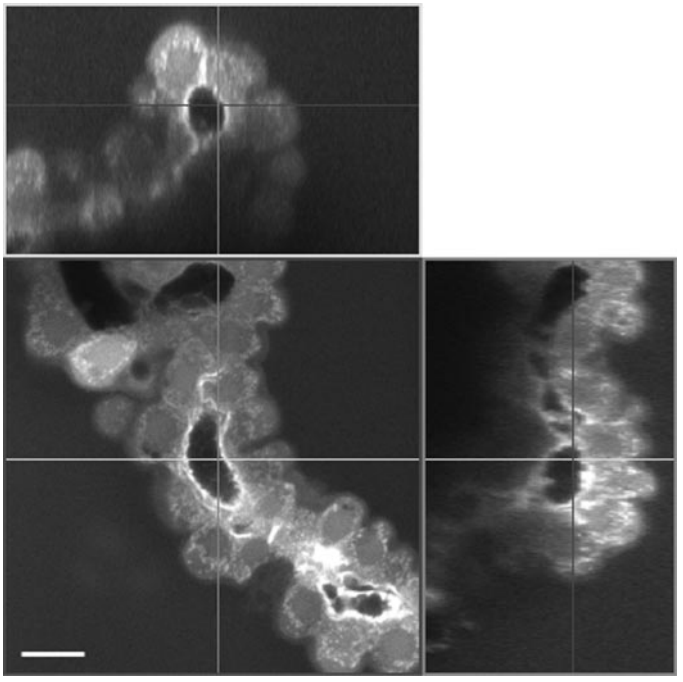

Fig. 2. Stack of confocal slices of rat choroid plexus. Tissue was incubated for 30 min in medium with 1 μM FL. A stack of 40 confocal images 0.5 μm apart was acquired, and *z*-sections through the stack were generated using Zeiss LSM 510 software. Figure shows the 21st *xy*-section at *center* and *z*-sections at the planes indicated *above* and at *right*.

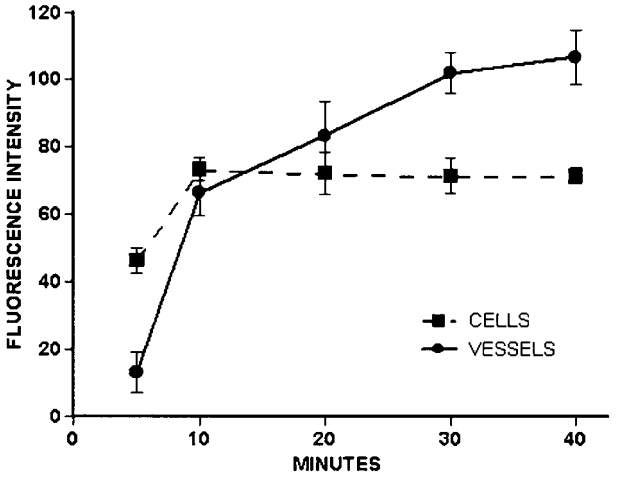

Fig. 4. Time course of uptake of 1 μM FL by choroid plexus tissue. Data given as means ± SE for 5 measurements of fluorescence intensity in cellular and vascular (vessel) spaces.

fluorescence decreased by 75%. Consistent with the indirect coupling mechanism, addition of 1–10 μM glutarate to the medium increased cellular and vascular fluorescence by 60–80% (Fig. 7). Thus FL uptake at the apical membrane and efflux into the vascular space were dependent on the Na^+ gradient and enhanced by dicarboxylate.

Nothing is known about the basolateral step in organic anion transport in choroid plexus. In renal proximal tubule, membrane vesicle studies indicate PD-driven facilitated diffusion in all species studied and anion exchange in some species (19), but experiments with intact tubules show no evidence of PD-driven transport (12, 24). To determine whether organic anion transport across the basolateral membrane of choroid plexus is PD driven, we increased the medium potassium concentration ($[K^+]$) 10-fold by replacing NaCl with KCl. This maneuver should have depolarized the cells and, because the tissue is a leaky epithelium that supports at most a small transpithelial PD, it should have depolarized both faces of the epithelial cells. Exposure to high-K^+ aCSF increased cellular fluorescence by 25% and decreased vascular fluorescence by 65% (Fig. 8*A*). As a result, the vessel-to-cell fluorescence-intensity ratio decreased from 2.6 ± 0.08 in control tissue to 0.7 ± 0.04 in high-K^+ tissue ($P < 0.01$). Note that in these experiments, we raised the medium K^+ level by replacing NaCl with KCl. Although FL transport is clearly Na^+ dependent, Fig. 6 shows that decreasing the aCSF Na^+ concentration by 51 mM had little effect on FL accumulation. Thus the effects of elevated aCSF $[K^+]$ that are seen in Fig. 8*A* cannot be attributed to reduced aCSF Na^+ concentration.

Although high K^+ levels appeared to affect the transport of FL from cell to vascular space substantially more than from aCSF to cell (Fig. 8), we wished to confirm the finding in an experiment in which uptake

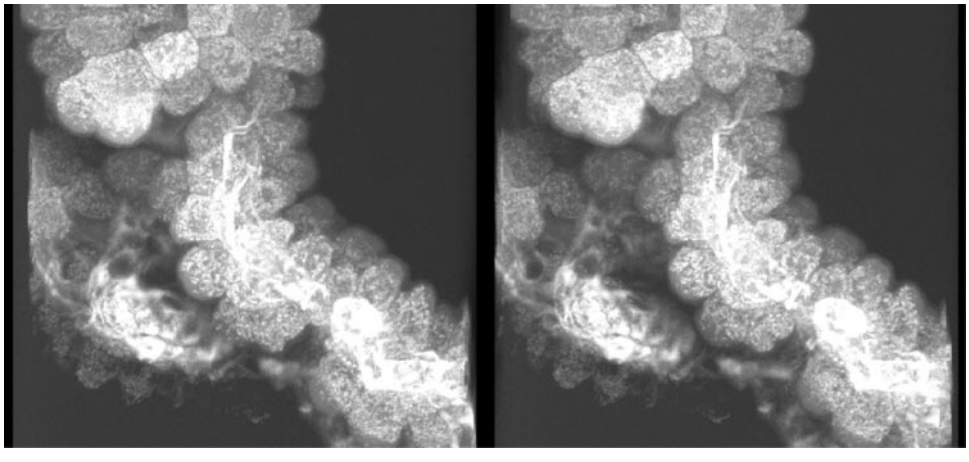

Fig. 3. Stereoimages of choroid plexus tissue reconstructed from the stack of confocal images used in Fig. 2. These are best viewed using a simple stereo viewer. This 3-dimensional reconstruction shows continuity of intensely fluorescent vascular and perivascular spaces as well as the distribution of punctate fluorescence throughout the cytoplasm of the epithelial cells.

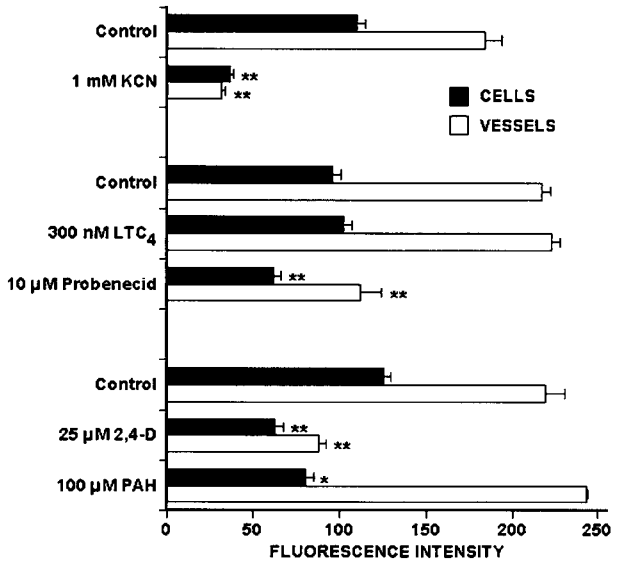

Fig. 5. Inhibition of FL accumulation in choroid plexus tissue by KCN and organic anions. Tissue was incubated in medium containing 1 μM FL without (control) or with the indicated additions. After 30 min, confocal images were acquired and analyzed as described in MATERIALS AND METHODS. Data are means ± SE for 5 measurements of fluorescence in cellular and vascular (vessel) spaces. $^{*}P < 0.05$, $^{**}P < 0.01$, significantly lower than control value. LTC_4, leukotriene C_4; PAH, *p*-aminohippurate

of substrate at the apical membrane was not a factor. To do this, we took advantage of CFDA, a nonfluorescent compound that enters cells by simple diffusion and is cleaved by esterases to produce the fluorescent organic anion carboxyfluorescein (CF). Previous imaging studies with renal proximal tubules showed that

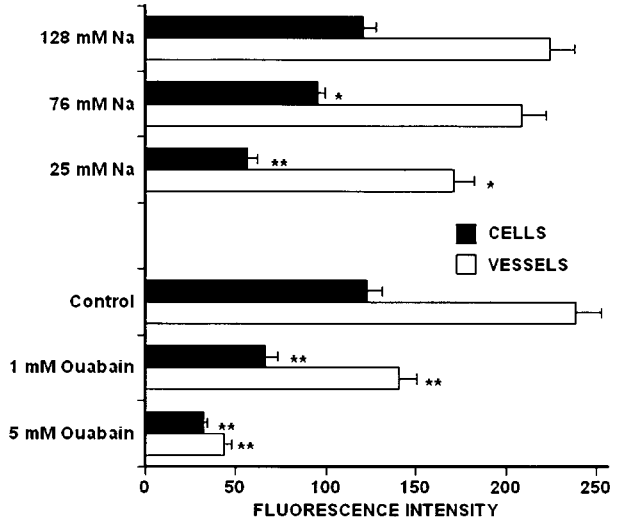

Fig. 6. Na^+ dependence and ouabain sensitivity of FL transport. *A*: tissue was incubated in medium containing 1 μM FL. Na^+ concentration was adjusted by replacing NaCl with *N*-methylglucamine. *B*: tissue was incubated in medium containing 1 μM FL without (control) or with the indicated concentration of ouabain. After 30 min, confocal images were acquired and analyzed as described in MATERIALS AND METHODS. Data are means ± SE for 5 measurements of fluorescence in cellular and vascular (vessel) spaces. $^{*}P < 0.05$, $^{**}P < 0.01$, significantly lower than control value.

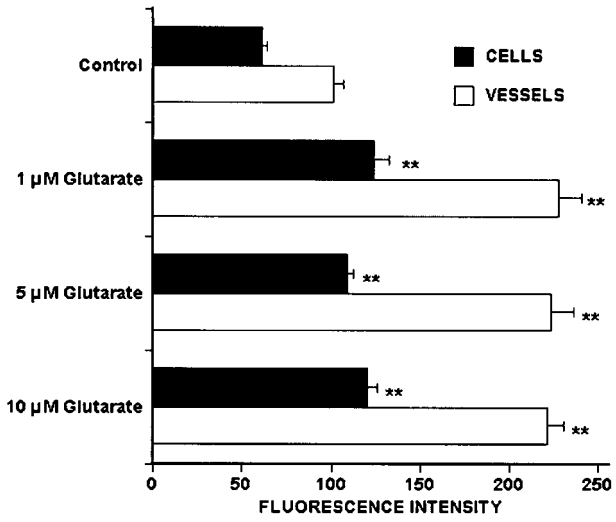

Fig. 7. Stimulation of FL transport by glutarate. Tissue was incubated in medium containing 1 μM FL without (control) or with the indicated concentration of glutarate. After 30 min, confocal images were acquired and analyzed as described in MATERIALS AND METHODS. Data given as means ± SE for 5 measurements of fluorescence in cellular and vascular (vessel) spaces. $^{**}P < 0.01$, significantly lower than control value.

CF transport from cell to tubular lumen was inhibited by PAH and probenecid but that transport was not PD dependent (12). When choroid plexus tissue was incubated in medium containing CFDA, CF accumulated in cells and perivascular/vascular spaces (Fig. 9*A*). In fact, the CF distribution pattern looked very much like

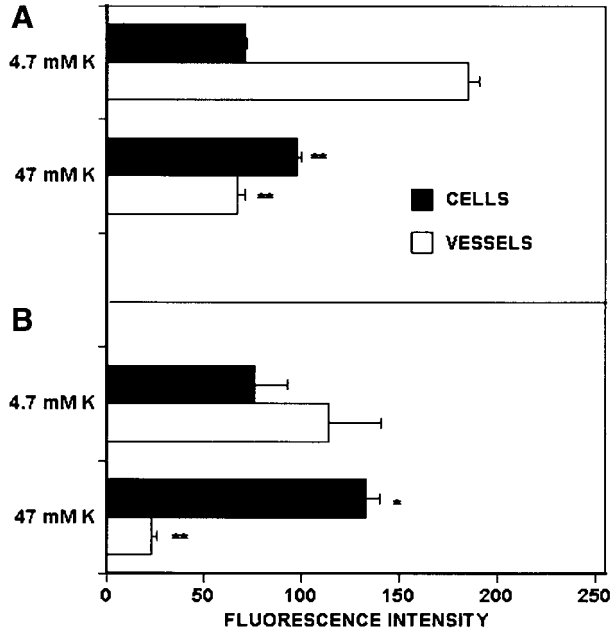

Fig. 8. Effect of elevated medium K^+ concentration ($[K^+]$) on FL (*A*) and carboxyfluorescein (CF; *B*) transport. Tissue was incubated in medium containing 1 μM FL or 5 μM carboxyfluorescein diacetate (CFDA) and the indicated concentration of K^+. After 30 min, confocal images were acquired and analyzed as described in MATERIALS AND METHODS. Data are means ± SE for 5 measurements of fluorescence in cellular and vascular (vessel) spaces. $^{*}P < 0.05$, $^{**}P < 0.01$, significantly lower than control value.

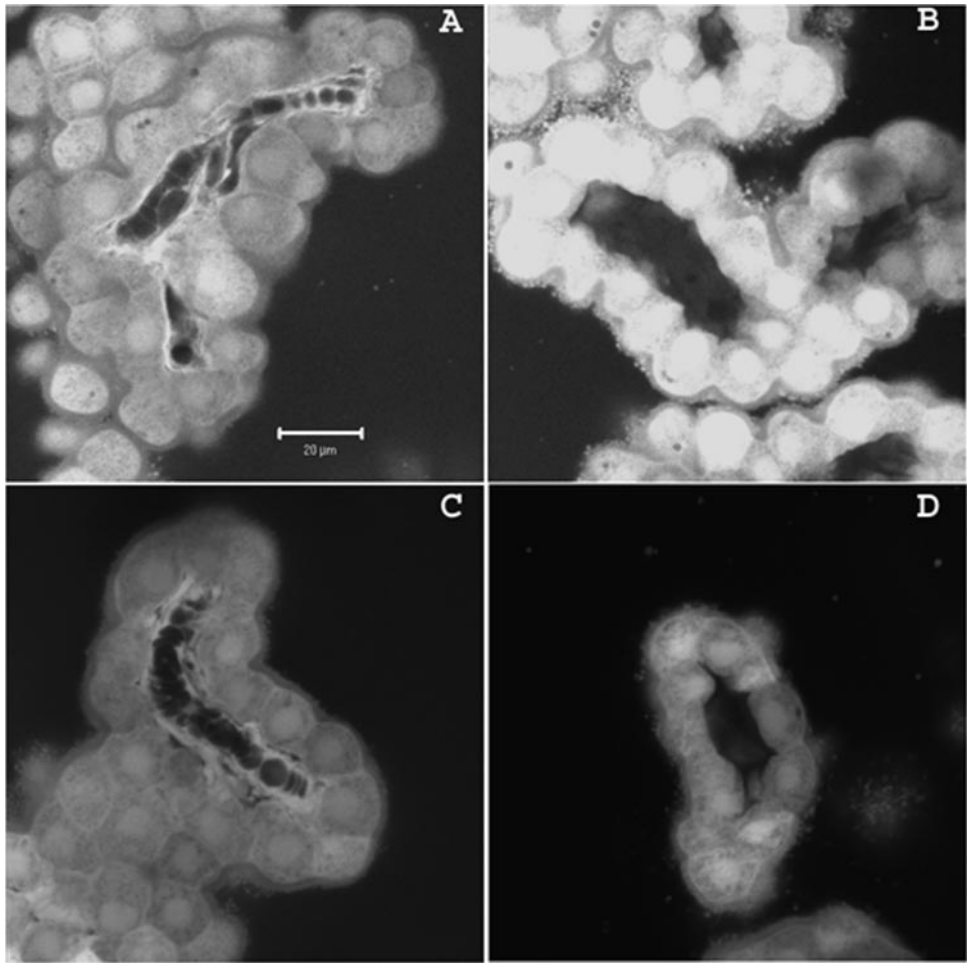

Fig. 9. Effect of 10 μM 2,4-dichlorophenoxyacetate (2,4-D) and elevated medium [K^+] on CF transport. Typical images from two experiments are shown. In the first experiment, tissue was incubated for 30 min in medium containing 1 μM CFDA without (control; *A*) or with (*B*) 10 μM 2,4-D. In the second experiment, tissue was incubated for 30 min in medium containing 1 μM CFDA and normal (4.7 mM; *C*) or high (47 mM; *D*) K^+. Scale bar, 20 μm.

that observed for FL. Addition of 10 μM 2,4-D to the medium reduced vascular accumulation of CF and increased cellular accumulation, which indicates specific transport out of the cell at the basolateral membrane and increasing accumulation of the enzymatically generated fluorescent organic anion when efflux was blocked (Fig. 9*B*). Incubation in high-K^+ aCSF increased CF fluorescence in cells and decreased CF fluorescence in the perivascular/vascular space (Figs. 8*B* and 9, *C* and *D*); high-K^+ medium reduced the vessel-to-cell fluorescence ratio from 1.5 ± 0.03 in controls to 0.23 ± 0.01 in high-K^+-treated tissue. These results are consistent with blocked efflux of CF at the basolateral membrane. Thus, for two fluorescent organic anions, one of which was generated intracellularly, transport out of the choroid plexus epithelial cells at the basolateral membrane was greatly reduced when the cells were depolarized with high K^+ levels.

It is interesting to compare the present confocal imaging results with those obtained using radiotracer techniques. In initial experiments, we found that the uptake of 10 μM [^{3}H]2,4-D by intact rat choroid plexus was rapid and reached a steady-state tissue-to-medium ratio of ~40 within 20 min (not shown). Figure 10 shows that in agreement with previous studies (7, 20) and the present imaging data, [^{3}H]2,4-D uptake (5-min initial rate) was concentrative and was reduced by unlabeled 2,4-D, Na^+ replacement, and ouabain. For present purposes, two new observations are particularly important. First, 10–100 μM FL inhibited 2,4-D uptake (Fig. 10). Because 2,4-D also inhibits FL uptake (see Fig. 5), these organic anions probably share a common pathway for uptake in choroid plexus. Second, incubating tissue in medium with high K^+ levels did not significantly affect 2,4-D uptake (Fig. 10). Because the imaging experiments showed that high K^+ levels tended to increase cellular accumulation of FL but to reduce vessel accumulation (see Figs. 8 and 9), the lack of effect of high-K^+ medium on [^{3}H]2,4-D uptake could indicate a similar pattern of largely offsetting effects. Clearly, the tracer-uptake data alone give no indication that high [K^+] could have such profound effects on organic anion distribution within the tissue.

DISCUSSION

The cells of the CNS are particularly sensitive to chemical injury and thus require a highly regulated extracellular environment. In this regard, the choroid plexus is a potent excretory system that transports xenobiotics and metabolic wastes from the CSF to the blood for eventual elimination in the urine and bile.

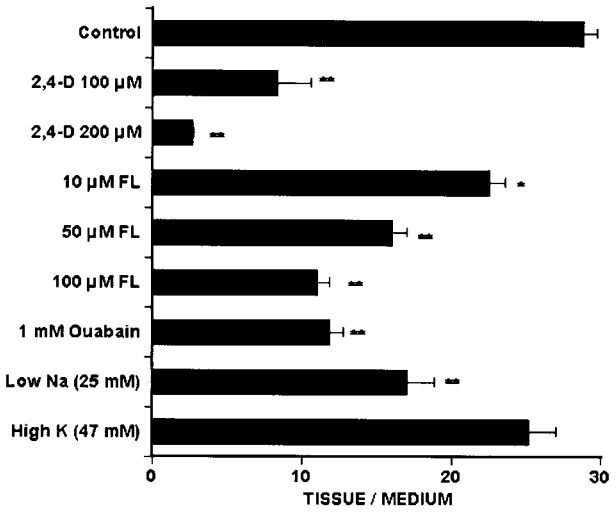

Fig. 10. Inhibition of 2,4-D uptake in rat choroid plexus. Intact choroid plexuses were incubated at 37°C in medium containing 10 μM [^{3}H]2,4-D without (control) or with the indicated modifications. After 5 min, tissue was removed, rinsed, and counted. Data are means ± SE for 6–12 choroid plexuses. *$P < 0.05$, **$P < 0.01$, significantly lower than control value.

Our understanding of the transport mechanisms by which choroid plexus does this is hampered by its small size, inaccessible location, and morphological complexity. To date, information about transport function in intact tissue has come from studies of solute movements in vivo and from drug-uptake experiments in vitro. Thus we have some understanding of the mechanisms that drive xenobiotic uptake at the apical membrane of the tissue but little information on subsequent steps. The present experiments describe a new approach to understanding mechanisms of transport in intact choroid plexus. We have used confocal microscopy and quantitative image analysis to follow the transport of FL, a fluorescent organic anion, across the intact, living, choroid plexus epithelium and into the underlying stroma and blood vessels. This approach provides the advantages of optical sectioning and spatial resolution down to the submicron level. As a result, we have been able to visualize and measure FL distribution within several compartments of the tissue and within the epithelial cells responsible for vectorial transport.

Steady-state FL distribution within choroid plexus tissue was not uniform. Relative to aCSF, all tissue compartments (with the possible exception of red cells) concentrated FL, but accumulation was higher in the interstitial/perivascular and vascular spaces than in the epithelial cells. Because fluorescence intensity increased from aCSF to epithelium to vascular space, transepithelial transport of FL must be the result of two uphill steps arranged in series with one at the apical plasma membrane and the other at the basolateral membrane.

The present data show that the first step is specific, coupled to metabolism, and Na^+ dependent. Cellular accumulation of FL was inhibited substantially by micromolar concentrations of the organic anions probenecid and 2,4-D and to a much smaller extent by PAH. Also, our data show that FL was a potent inhibitor of 2,4-D accumulation in rat choroid plexus slices, which suggests that the two organic anions share a common transport pathway. However, LTC_4 had no effect on FL transport, which indicates that multidrug resistance proteins (MRPs) and organic ion transport proteins (OATPs), transporters that are expressed in choroid plexus but that generally handle larger organic anions, were not involved in the transport of FL. In this regard, recent studies certainly provide evidence for these transporters playing an important role in the handling of other xenobiotics by choroid plexus (5, 6, 8, 17, 28).

The present data show that transport of FL (cellular and vascular accumulation) decreased when metabolism was inhibited by KCN, when bath Na^+ was reduced from 130 to 26 mM, and when the tissue was exposed to ouabain. Moreover, accumulation increased by >50% when 1–10 μM glutarate was added to the bath. This pattern of effects is identical to the one obtained in studies of radiolabeled 2,4-D accumulation in rat choroid plexus (Refs. 7, 20, and the present study) and is consistent with at least a portion of FL uptake being mediated by OAT1 through FL/dicarboxylate exchange and Na^+-dicarboxylate cotransport as in renal proximal tubule (19).

Note that with each of these treatments, we found parallel changes in FL accumulation in the epithelial cells, interstitial/perivascular spaces, and blood vessels. That is, as with cells, accumulation in vessels decreased with competitor organic anions, KCN, and low Na^+ and ouabain levels, and increased with glutarate. Thus, as in renal proximal tubule (19), the first step in transport, i.e., indirect coupling of organic anion uptake to Na^+ at the apical membrane of choroid plexus, drives not only cellular accumulation but also transepithelial transport.

Confocal imaging has allowed us for the first time to visualize and explore the second step in transport: efflux at the basolateral membrane. We tested whether this step was PD sensitive by determining the effect on transport of increasing the medium [K^+] by 10-fold. This maneuver should have depolarized the apical membrane and, because the tissue is a leaky epithelium that supports at most a small transepithelial PD, it should have also depolarized the basolateral membrane. In a primary culture of neonatal rat choroid plexus cells, a similar increase in medium [K^+] depolarized the PD by 40 mV (27). In the present study, increasing the medium [K^+] reduced vessel accumulation of FL but increased cellular FL. As a result, the lumen-to-cell fluorescence ratio decreased from 2.6 to 0.6. This is the only treatment that reduced this ratio below unity, which suggests an effect on basolateral efflux that could not be accounted for by the smaller reduction in cellular accumulation.

To further characterize the efflux step, we used CFDA as substrate. This compound is uncharged and membrane permeant. Within cells, it is hydrolyzed to CF, a fluorescent organic anion. Thus the use of CFDA allowed us to bypass the entry step at the apical mem-

brane and focus on organic anion efflux at the basolateral membrane. CF efflux was clearly mediated, because it was blocked by 2,4-D. Moreover, as with FL, increasing medium [K^+] also blocked CF efflux at the basolateral membrane. It is unlikely that the high-K^+ medium reduced FL and CF transport by inhibiting cell metabolism or opening tight junctions, because uphill transport of the large organic anions, Texas red free acid, and FL-methotrexate was not decreased when medium [K^+] was increased (D. S. Miller, unpublished observations). These compounds must exit choroid plexus epithelial cells by a mechanism that is different from the one used by the smaller organic anions FL and CF. Thus, for the two small organic anions tested, FL and CF, depolarization reduced cell-to-vessel transport, which indicates PD-driven efflux at the basolateral membrane.

The present confocal-imaging study has also opened a window on the distribution of organic anions within choroid plexus epithelial cells. The images show that FL was distributed in diffuse and punctate compartments and that punctate fluorescence was substantially higher than diffuse cytoplasmic fluorescence. A similar distribution was found in renal tissue that transports organic anions (opossum kidney cells and intact teleost proximal tubules), where FL concentrated in vesicles that moved by a microtubule-dependent mechanism and where vesicle-mediated transport appeared to contribute to net secretion (14, 15). In addition, an endosome-based mechanism has been proposed to contribute to organic cation transport in kidney and choroid plexus (16, 21). Whether vesicle-mediated mechanisms contribute to organic anion transport in choroid plexus is a focus of current experiments.

As in renal proximal tubule (2, 25), we are now developing at the cellular and molecular levels a mechanistic understanding of the processes that drive excretory transport of small organic anions from CSF to blood in choroid plexus. Recent studies have identified OAT1 (20) and OAT3 (9) as being expressed in the tissue. rOAT1 appears to be targeted to the apical membrane of rat choroid plexus epithelial cells, and OAT1 is the only member of the OAT subfamily of transporters with demonstrated energetic coupling to the Na^+ gradient (25). Based on these characteristics and the present results for FL, rOAT1 is one likely candidate for the transporter mediating apical uptake in choroid plexus.

We know considerably less about OAT3 localization and function. The rat and human forms of this transporter have been cloned (3, 9). When expressed in *Xenopus* oocytes, hOAT3 and rOAT3 clearly have wider specificity profiles than hOAT1 or rOAT1. For both species, OAT3 mRNA has been detected in brain and possibly in choroid plexus. In kidney, hOAT3 has been immunolocalized to the basolateral membrane of proximal tubules, where it along with hOAT1 could mediate organic anion uptake (3).

At present, it is not clear how transport on OAT3 is coupled to cellular metabolism, which is an important issue if this transporter is responsible for driving organic anions into renal proximal tubule and choroid plexus epithelial cells. Estrone sulfate transport on rOAT3 and hOAT3 was not Na^+ dependent and was not *trans*-stimulated by any of the organic anions tested (3, 9). Nevertheless, if OAT3 were localized to the apical membrane of choroid plexus epithelial cells, it could provide a second pathway for organic anion uptake as suggested by Kusuhara and colleagues (9). It remains to be demonstrated whether this pathway exhibits indirect coupling to Na^+, a characteristic of the uptake of FL (present study) and 2,4-D (20) in choroid plexus. Alternatively, if OAT3 were on the basolateral membrane of choroid plexus epithelial cells and if it were capable of PD-driven transport, it could mediate organic anion efflux. Clearly, additional studies are needed to complete at the molecular level identification of the transporters responsible for organic anion transport across choroid plexus.

Finally, as with renal proximal tubules (11) and brain capillaries (13), the present study again demonstrates the power of quantitative fluorescence-based microscopic techniques to probe intact living-tissue transport mechanisms at the cellular and subcellular levels. Confocal imaging provides information about spatiotemporal aspects of vectorial transport that cannot be obtained with more traditional radiotracer and molecular techniques. The challenge is to be able to use imaging with the other techniques to build detailed models of transport that will help us understand function and regulation at multiple organizational levels.

REFERENCES

1. **Bresler SE, Bresler VM, Kazbekov EN, Nikiforov AA, and Vasilieva NN.** On the active transport of organic acids (fluorescein) in the choroid plexus of the rabbit. *Biochim Biophys Acta* 550: 110–119, 1979.
2. **Burckhardt G and Wolff NA.** Structure of renal organic anion and cation transporters. *Am J Physiol Renal Physiol* 278: F853–F866, 2000.
3. **Cha SH, Sekine T, Fukushima JI, Kanai Y, Kobayashi Y, Goya T, and Endou H.** Identification and characterization of human organic anion transporter 3 expressing predominantly in the kidney. *Mol Pharmacol* 59: 1277–1286, 2001.
4. **Cserr HF and VanDyke DH.** 5-Hydroxyindoleacetic acid accumulation by isolated choroid plexus. *Am J Physiol* 220: 718–723, 1971.
5. **Gao B, Hagenbuch B, Kullak-Ublick GA, Benke D, Aguzzi A, and Meier PJ.** Organic anion-transporting polypeptides mediate transport of opioid peptides across blood-brain barrier. *J Pharmacol Exp Ther* 294: 73–79, 2000.
6. **Gao B and Meier PJ.** Organic anion transport across the choroid plexus. *Microsc Res Tech* 52: 60–64, 2001.
7. **Kim CS and Pritchard JB.** Transport of 2,4,5-trichlorophenoxyacetic acid across the blood-cerebrospinal fluid barrier of the rabbit. *J Pharmacol Exp Ther* 267: 751–757, 1993.
8. **Konig J, Nies AT, Cui Y, Leier I, and Keppler D.** Conjugate export pumps of the multidrug resistance protein (MRP) family: localization, substrate specificity, and MRP2-mediated drug resistance. *Biochim Biophys Acta* 1461: 377–394, 1999.
9. **Kusuhara H, Sekine T, Utsunomiya-Tate N, Tsuda M, Kojima R, Cha SH, Sugiyama Y, Kanai Y, and Endou H.** Molecular cloning and characterization of a new multispecific organic anion transporter from rat brain. *J Biol Chem* 274: 13675–13680, 1999.
10. **Masereeuw R, Moons MM, Toomey BH, Russel FG, and Miller DS.** Active lucifer yellow secretion in renal proximal

tubule: evidence for organic anion transport system crossover. *J Pharmacol Exp Ther* 289: 1104–1111, 1999.
11. **Masereeuw R, Russel FG, and Miller DS.** Multiple pathways of organic anion secretion in renal proximal tubule revealed by confocal microscopy. *Am J Physiol Renal Fluid Electrolyte Physiol* 271: F1173–F1182, 1996.
12. **Miller DS, Letcher S, and Barnes DM.** Fluorescence imaging study of organic anion transport from renal proximal tubule cell to lumen. *Am J Physiol Renal Fluid Electrolyte Physiol* 271: F508–F520, 1996.
13. **Miller DS, Nobmann SN, Gutmann H, Toeroek M, Drewe J, and Fricker G.** Xenobiotic transport across isolated brain microvessels studied by confocal microscopy. *Mol Pharmacol* 58: 1357–1367, 2000.
14. **Miller DS and Pritchard JB.** Nocodazole inhibition of organic anion secretion in teleost renal proximal tubules. *Am J Physiol Regulatory Integrative Comp Physiol* 267: R695–R704, 1994.
15. **Miller DS, Stewart DE, and Pritchard JB.** Intracellular compartmentation of organic anions within renal cells. *Am J Physiol Regulatory Integrative Comp Physiol* 264: R882–R890, 1993.
16. **Miller DS, Villalobos AR, and Pritchard LB.** Organic cation transport in rat choroid plexus cells studied by fluorescence microscopy. *Am J Physiol Cell Physiol* 276: C955–C968, 1999.
17. **Nishino J, Suzuki H, Sugiyama D, Kitazawa T, Ito K, Hanano M, and Sugiyama Y.** Transepithelial transport of organic anions across the choroid plexus: possible involvement of organic anion transporter and multidrug resistance-associated protein. *J Pharmacol Exp Ther* 290: 289–294, 1999.
18. **Pritchard JB.** Accumulation of anionic pesticides by rabbit choroid plexus in vitro. *J Pharmacol Exp Ther* 212: 354–359, 1980.
19. **Pritchard JB and Miller DS.** Mechanisms mediating renal secretion of organic anions and cations. *Physiol Rev* 73: 765–796, 1993.
20. **Pritchard JB, Sweet DH, Miller DS, and Walden R.** Mechanism of organic anion transport across the apical membrane of choroid plexus. *J Biol Chem* 274: 33382–33387, 1999.
21. **Pritchard JB, Sykes DB, Walden R, and Miller DS.** ATP-dependent transport of tetraethylammonium by endosomes isolated from rat renal cortex. *Am J Physiol Renal Fluid Electrolyte Physiol* 266: F966–F976, 1994.
22. **Suzuki H, Sawada Y, Sugiyama Y, Iga T, and Hanano M.** Anion exchanger mediates benzylpenicillin transport in rat choroid plexus. *J Pharmacol Exp Ther* 243: 1147–1152, 1987.
23. **Suzuki H, Sawada Y, Sugiyama Y, Iga T, and Hanano M.** Transport of benzylpenicillin by the rat choroid plexus in vitro. *J Pharmacol Exp Ther* 242: 660–665, 1987.
24. **Ullrich KJ and Rumrich G.** Luminal transport step of para-aminohippurate (PAH): transport from PAH-loaded proximal tubular cells into the tubular lumen of the rat kidney in vivo. *Pflügers Arch* 433: 735–743, 1997.
25. **Van Aubel RA, Masereeuw R, and Russel FG.** Molecular pharmacology of renal organic anion transporters. *Am J Physiol Renal Physiol* 279: F216–F232, 2000.
26. **van Dyke DH, Cserr H, and Barlow CF.** 5-Hydroxyindoleacetic acid (5-HIAA) transport by isolated choroid plexus. *Neurology* 20: 393–394, 1970.
27. **Villalobos AR, Parmelee JT, and Renfro JL.** Choline uptake across the ventricular membrane of neonate rat choroid plexus. *Am J Physiol Cell Physiol* 276: C1288–C1296, 1999.
28. **Wijnholds J, deLange EC, Scheffer GL, van den Berg DJ, Mol CA, van der Valk M, Schinkel AH, Scheper RJ, Breimer DD, and Borst P.** Multidrug resistance protein 1 protects the choroid plexus epithelium and contributes to the blood-cerebrospinal fluid barrier. *J Clin Invest* 105: 279–285, 2000.